The ASAS-SN Bright Supernova Catalog – III. 2016

T. W.-S. Holoien[1,2,3⋆], J. S. Brown[1], K. Z. Stanek[1,2], C. S. Kochanek[1,2], B. J. Shappee[4,5], J. L. Prieto[6,7], Subo Dong[8], J. Brimacombe[9], D. W. Bishop[10], S. Bose[8], J. F. Beacom[1,2,11], D. Bersier[12], Ping Chen[8], L. Chomiuk[13], E. Falco[14], D. Godoy-Rivera[1], N. Morrell[15], G. Pojmanski[16], J. V. Shields[1], J. Strader[13], M. D. Stritzinger[17], Todd A. Thompson[1,2], P. R. Woźniak[18], G. Bock[19], P. Cacella[20], E. Conseil[21], I. Cruz[22], J. M. Fernandez[23], S. Kiyota[24], R. A. Koff[25], G. Krannich[26], P. Marples[27], G. Masi[28], L. A. G. Monard[29], B. Nicholls[30], J. Nicolas[31], R. S. Post[32], G. Stone[33], and W. S. Wiethoff[34]

[1] *Department of Astronomy, The Ohio State University, 140 West 18th Avenue, Columbus, OH 43210, USA*
[2] *Center for Cosmology and AstroParticle Physics (CCAPP), The Ohio State University, 191 W. Woodruff Ave., Columbus, OH 43210, USA*
[3] *US Department of Energy Computational Science Graduate Fellow*
[4] *Carnegie Observatories, 813 Santa Barbara Street, Pasadena, CA 91101, USA*
[5] *Hubble and Carnegie-Princeton Fellow*
[6] *Núcleo de Astronomía de la Facultad de Ingeniería y Ciencias, Universidad Diego Portales, Av. Ejército 441, Santiago, Chile*
[7] *Millennium Institute of Astrophysics, Santiago, Chile*
[8] *Kavli Institute for Astronomy and Astrophysics, Peking University, Yi He Yuan Road 5, Hai Dian District, Beijing 100871, China*
[9] *Coral Towers Observatory, Cairns, Queensland 4870, Australia*
[10] *Rochester Academy of Science, 1194 West Avenue, Hilton, NY 14468, USA*
[11] *Department of Physics, The Ohio State University, 191 W. Woodruff Ave., Columbus, OH 43210, USA*
[12] *Astrophysics Research Institute, Liverpool John Moores University, 146 Brownlow Hill, Liverpool L3 5RF, UK*
[13] *Department of Physics and Astronomy, Michigan State University, East Lansing, MI 48824, USA*
[14] *Harvard-Smithsonian Center for Astrophysics, 60 Garden St., Cambridge, MA 02138, USA*
[15] *Las Campanas Observatory, Carnegie Observatories, Casilla 601, La Serena, Chile*
[16] *Warsaw University Astronomical Observatory, Al. Ujazdowskie 4, 00-478 Warsaw, Poland*
[17] *Department of Physics and Astronomy, Aarhus University, Ny Munkegade 120, DK-8000 Aarhus C, Denmark*
[18] *Los Alamos National Laboratory, Mail Stop B244, Los Alamos, NM 87545, USA*
[19] *Runaway Bay Observatory, 1 Lee Road, Runaway Bay, Queensland 4216, Australia*
[20] *DogsHeaven Observatory, SMPW Q25 CJ1 LT10B, Brasilia, DF 71745-501, Brazil*
[21] *Association Francaise des Observateurs d'Etoiles Variables (AFOEV), Observatoire de Strasbourg, 11 Rue de l'Universite, 67000 Strasbourg, France*
[22] *Cruz Observatory, 1971 Haverton Drive, Reynoldsburg, OH 43068, USA*
[23] *Observatory Inmaculada del Molino, Hernando de Esturmio 46, Osuna, 41640 Sevilla, Spain*
[24] *Variable Star Observers League in Japan, 7-1 Kitahatsutomi, Kamagaya, Chiba 273-0126, Japan*
[25] *Antelope Hills Observatory, 980 Antelope Drive West, Bennett, CO 80102, USA*
[26] *Roof Observatory Kaufering, Lessingstr. 16, D-86916 Kaufering, Germany*
[27] *Leyburn & Loganholme Observatories, 45 Kiewa Drive, Loganholme, Queensland 4129, Australia*
[28] *Virtual Telescope Project, Via Madonna de Loco, 47-03023 Ceccano (FR), Italy*
[29] *Kleinkaroo Observatory, Calitzdorp, St. Helena 1B, P.O. Box 281, 6660 Calitzdorp, Western Cape, South Africa*
[30] *Mount Vernon Observatory, 6 Mount Vernon Place, Nelson, New Zealand*
[31] *Groupe SNAude France, 364 Chemin de Notre Dame, 06220 Vallauris, France*
[32] *Post Observatory, Lexington, MA 02421, USA*
[33] *Sierra Remote Observatories, 44325 Alder Heights Road, Auberry, CA 93602, USA*
[34] *Department of Earth and Environmental Sciences, University of Minnesota, 230 Heller Hall, 1114 Kirby Drive, Duluth, MN. 55812, USA*

arXiv:1704.02320v1 [astro-ph.HE] 7 Apr 2017

11 April 2017

ABSTRACT

This catalog summarizes information for all supernovae discovered by the All-Sky Automated Survey for SuperNovae (ASAS-SN) and all other bright ($m_{peak} \leqslant 17$), spectroscopically confirmed supernovae discovered in 2016. We then gather the near-IR through UV magnitudes of all host galaxies and the offsets of the supernovae from the centers of their hosts from public databases. We illustrate the results using a sample that now totals 668 supernovae discovered since 2014 May 1, including the supernovae from our previous catalogs, with type distributions closely matching those of the ideal magnitude limited sample from Li et al. (2011). This is the third of a series of yearly papers on bright supernovae and their hosts from the ASAS-SN team.

Key words: supernovae, general — catalogues — surveys

© 2017 The Authors

1 INTRODUCTION

The last two decades have seen the proliferation of large, systematic surveys that search some or all of the sky for supernovae (SNe) and other transient phenomena. Significant examples include the Lick Observatory Supernova Search (LOSS; Li et al. 2000), the Panoramic Survey Telescope & Rapid Response System (Pan-STARRRS; Kaiser et al. 2002), the Texas Supernova Search (Quimby 2006), the Sloan Digital Sky Survey (SDSS) Supernova Survey (Frieman et al. 2008), the Catalina Real-Time Transient Survey (CRTS; Drake et al. 2009), the CHilean Automatic Supernova sEarch (CHASE; Pignata et al. 2009), the Palomar Transient Factory (PTF; Law et al. 2009), the Gaia transient survey (Hodgkin et al. 2013), the La Silla-QUEST (LSQ) Low Redshift Supernova Survey (Baltay et al. 2013), the Mobile Astronomical System of TElescope Robots (MASTER; Gorbovskoy et al. 2013) survey, the Optical Gravitational Lensing Experiment-IV (OGLE-IV; Wyrzykowski et al. 2014), and the Asteroid Terrestrial-impact Last Alert System (ATLAS; Tonry 2011).

Despite the number of transient survey projects, there has been no rapid-cadence optical survey scanning the entire visible sky to find the bright and nearby transients that can be observed in the greatest detail. Such events can provide the detailed observational data needed to have the greatest physical impact.

This is the goal of the All-Sky Automated Survey for SuperNovae (ASAS-SN[1]; Shappee et al. 2014). ASAS-SN is a long-term project designed to find bright transients, and has been highly successful since the beginning of survey operations, finding many interesting and nearby supernovae (e.g., Dong et al. 2016a; Holoien et al. 2016b; Shappee et al. 2016a; Godoy-Rivera et al. 2017), tidal disruption events (Holoien et al. 2014a; Brown et al. 2016b,a; Holoien et al. 2016d,c; Prieto et al. 2016a; Romero-Cañizales et al. 2016), active galactic nucleus flares (Shappee et al. 2014), stellar outbursts (Holoien et al. 2014b; Schmidt et al. 2014; Herczeg et al. 2016; Schmidt et al. 2016), and cataclysmic variable stars (Kato et al. 2014a,b, 2015, 2016).

During 2016, ASAS-SN comprised eight 14-cm telescopes with standard V-band filters, each with a 4.5×4.5 degree field-of-view and a limiting magnitude of $m_V \sim 17$ (see Shappee et al. (2014) for further technical details). These telescopes are divided into two units each with four telescopes on a common mount hosted by the Las Cumbres Observatory (LCO; Brown et al. 2013). Brutus, our northern unit, is housed at the LCO site on Mount Haleakala in Hawaii, and Cassius, our southern unit, is hosted at the LCO site at Cerro Tololo, Chile. The two units combined give ASAS-SN roughly 20000 square degrees of coverage per clear night, allowing us to cover the entire observable sky (roughly 30000 square degrees at any given time) with a $2-3$ day cadence. In 2017, ASAS-SN will expand to five units (20 telescopes) at four sites (Hawaii, McDonald Observatory in Texas, Sutherland, South Africa, and two in Chile), allowing nightly coverage of the visible sky with little sensitivity to local weather. For a more detailed history of the ASAS-SN project, see the introduction of Holoien et al. (2016a) and Shappee et al. (2014).

[1] http://www.astronomy.ohio-state.edu/~assassin/

ASAS-SN data are processed and searched in real-time and all ASAS-SN discoveries are announced publicly upon confirmation, allowing for rapid discovery and response by both the ASAS-SN team and others. Our untargeted survey approach and complete spectroscopic identification makes our sample less biased than those of many other supernova searches. This makes it ideal for population studies of nearby supernovae and their hosts.

This manuscript is the third of a series of yearly catalogs provided by the ASAS-SN team and presents collected information on supernovae discovered by ASAS-SN in 2016 and their host galaxies. As in our previous catalogs (Holoien et al. 2016a, 2017), we also provide the same information for bright supernovae (those with $m_{peak} \leqslant 17$) that were discovered by other professional surveys and amateur astronomers in 2016 to construct a complete sample of bright supernovae discovered in 2016. This includes whether ASAS-SN independently found the supernovae after the initial announcement.

The analyses and information presented in this paper supersede the information presented in discovery and classification Astronomer's Telegrams (ATels), which we cite in this manuscript, and the information publicly available on ASAS-SN webpages and the Transient Name Server (TNS[2]).

In §2 we describe the sources of the information presented in this manuscript and list ASAS-SN supernovae with updated classifications or redshift measurements. In §3, we give statistics on the supernova and host galaxy populations in our full cumulative sample, including the discoveries listed in Holoien et al. (2016a, 2017), and discuss overall trends in the sample. Throughout our analyses, we assume a standard ΛCDM cosmology with $H_0 = 69.3$ km s^{-1} Mpc^{-1}, $\Omega_M = 0.29$, and $\Omega_\Lambda = 0.71$ for converting host redshifts into distances. In §4, we conclude with our overall findings and discuss how the upcoming expansion to ASAS-SN will impact our future discoveries.

2 DATA SAMPLES

Below we outline the sources of the data collected in our supernova and host galaxy samples. These data are presented in Tables 1, 2, 3, and 4.

2.1 The ASAS-SN Supernova Sample

Table 1 includes information for all supernovae discovered by ASAS-SN between 2016 January 1 and 2016 December 31. As in Holoien et al. (2016a, 2017), all names, discovery dates, and host names are taken from our discovery ATels, all of which are cited in Table 1. We also include the supernova names designated by TNS, the official IAU mechanism for reporting new astronomical transients. As is noted in our ATels, the ASAS-SN team is participating in the TNS system to minimize potential confusion, but we use the ASAS-SN designations as our primary nomenclature and encourage others to do the same in order to preserve the origin of the transient in future literature.

ASAS-SN supernova redshifts were spectroscopically

[2] https://wis-tns.weizmann.ac.il/

measured from classification spectra. For those cases where a supernova host had a previously measured redshift and the host redshift is consistent with the transient redshift, we list the redshift of the host taken from the NASA/IPAC Extragalactic Database (NED)[3]. For all other cases we typically report the redshifts given in the classification telegrams, excepting those that have been updated in this work (see below).

ASAS-SN supernova classifications are taken from classification telegrams, which we have cited in Table 1, when available. In some cases a classification was only reported on TNS and was not reported in an ATel; for these cases we list "TNS" in the "Classification Telegram" column. When available in the classification ATel or on TNS we also give the approximate age at discovery measured in days relative to peak. Classifications were typically obtained using either the Supernova Identification code (SNID; Blondin & Tonry 2007) or the Generic Classification Tool (GELATO[4]; Harutyunyan et al. 2008), which both compare observed input spectra to template spectra in order to estimate the supernova age and type.

Using archival classification and late-time spectra of the ASAS-SN supernova discoveries taken from TNS and Weizmann Interactive Supernova data REPository (WISEREP; Yaron & Gal-Yam 2012), we also update a number of redshifts and classifications that differ from what was reported in the discovery and classification telegrams. ASASSN-16ah, ASASSN-16bm, ASASSN-16bq, ASASSN-16bv, ASASSN-16cr, ASASSN-16cs, ASASSN-16es, ASASSN-16fa, ASASSN-16fc, ASASSN-16fx, ASASSN-16gz, ASASSN-16hr, ASASSN-16hw, ASASSM-16ip, ASASSN-16je, ASASSN-16jj, ASASSN-16la, ASASSN-16lc, ASASSN-16ll, ASASSN-16mj, ASASSN-16ns, ASASSN-16oj, ASASSN-16ok, ASASSN-16ol, ASASSN-16oy, ASASSN-16pd, ASASSN-16pj, and ASASSN-16pk have updated redshifts based on archival spectra. ASASSN-16dx has been reclassified from archival spectra, and ASASSN-16fp has been classified as a Ib/Ic-BL (Yamanaka et al. 2017). All updated redshifts and classifications are reported in Table 1.

Using the astrometry.net (Barron et al. 2008; Lang et al. 2010) package we solved the astrometry in follow-up images for all ASAS-SN supernovae and measured a centroid position for the supernova using IRAF. This approach typically yields errors of $<1\farcs0$ in position, which is significantly more accurate than measuring the supernova position directly in ASAS-SN images, which have a $7\farcs0$ pixel scale. The images used to measure astrometry were obtained using the LCO 1-m telescopes (Brown et al. 2013), OSMOS mounted on the MDM Hiltner 2.4-m telescope, or from amateur collaborators working with the ASAS-SN team. For most cases, the coordinates measured from follow-up images were reported in our discovery ATels, but we report new, more accurate coordinates in Table 1 for those cases where the supernovae were announced with coordinates measured in ASAS-SN data. The offset from the host galaxy nucleus is also reported, and was calculated using the coordinates measured from follow-up images and host coordinates available in NED.

[3] https://ned.ipac.caltech.edu/
[4] gelato.tng.iac.es

V-band, host-subtracted discovery and peak magnitudes were re-measured from ASAS-SN data for all ASAS-SN supernova discoveries, and these magnitudes are reported in Table 1. This has resulted in differences between the magnitudes reported in this work and the magnitudes reported in the original discovery ATels for some cases, where re-reduction of the data has led to improvements in our photometry. We define the "discovery magnitude" as the magnitude of the supernova on the announced discovery date. For cases with enough detections in the light curve, we also perform a parabolic fit to the light curve and estimate a peak magnitude based on the fit. The "peak magnitude" reported in Table 1 is the brighter value between the brightest measured magnitude and the peak of the parabolic fit.

We include all supernovae discovered by ASAS-SN in 2016 in this catalog and in Table 1, including those that peaked at magnitudes fainter than $m_V = 17$. In the comparison analyses presented in §3, however, we only include those ASAS-SN supernovae with $m_{V,peak} \leqslant 17$ so that our sample is consistent with the non-ASAS-SN sample.

2.2 The Non-ASAS-SN Supernova Sample

In Table 2 we give information for all spectroscopically confirmed supernovae with peak magnitudes of $m_{peak} \leqslant 17$ that were discovered by other professional and amateur supernova searches between 2016 January 1 and 2016 December 31.

We compiled data for the non-ASAS-SN discoveries from the "latest supernovae" website[5] designed and maintained by D. W. Bishop (Gal-Yam et al. 2013). This site compiles discoveries reported from different channels and links objects reported by different sources at different times, making it an ideal source for collecting information on supernovae discovered by different search groups. While we did use TNS for verification of the data from the latest supernovae website, we did not use it as the primary source of information on non-ASAS-SN discoveries, as some supernova searches do not participate in the TNS system.

Names, IAU names, discovery dates, coordinates, host names, host offsets, peak magnitudes, spectral types, and discovery sources for each supernova in the non-ASAS-SN sample were taken from the latest supernovae website when possible. Host galaxy redshifts were collected from NED when available and were taken from the latest supernovae website otherwise. For cases where a host name or host offset was not listed on the website for a supernova, the primary name and offset were taken from NED. In these cases, we define the offset as the distance between the reported coordinates of the supernova and the galaxy coordinates in NED. In some cases, no catalogued galaxy was listed at the position of the host in NED, but a host galaxy was clearly visible in archival Pan-STARRS data (Chambers et al. 2016) . In these cases, we measured the centroid position of the host nucleus using IRAF and calculated the offset using those coordinates. For all supernovae in both samples we use the primary name of the host galaxy listed in NED, which sometimes differs from the name listed on the ASAS-SN supernova page or the latest supernova website.

[5] http://www.rochesterastronomy.org/snimages/

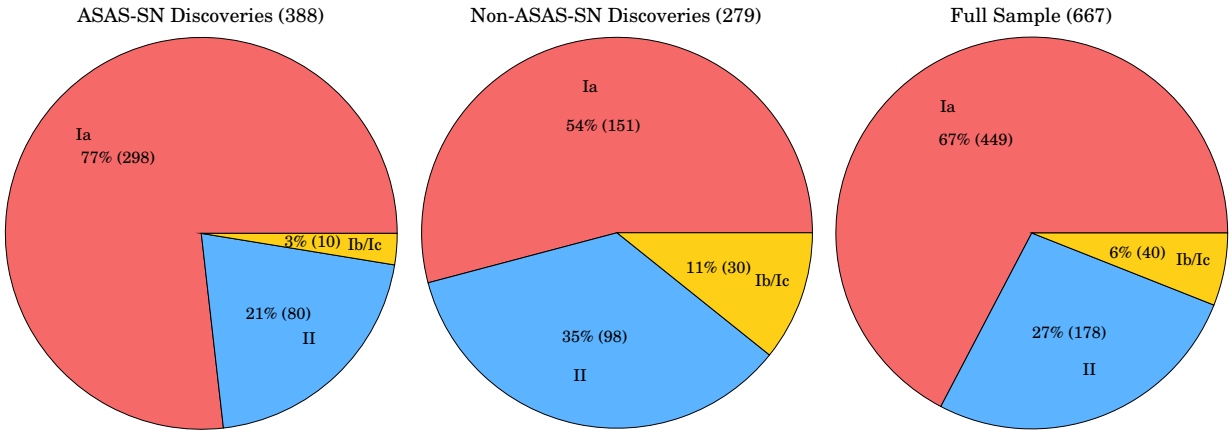

Figure 1. *Left Panel*: Breakdown by type of the supernovae discovered by ASAS-SN between 2014 May 01 and 2016 December 31. The proportions of each type is very similar to that of an ideal magnitude-limited sample (Li et al. 2011). *Center Panel*: The same chart for the non-ASAS-SN sample in the same time period. *Right Panel*: The same breakdown of types for the combined supernova sample. For the purposes of this analysis, we exclude superluminous supernovae and include Type IIb supernovae in the "Type II" sample.

We update the redshifts and classifications of several supernovae discovered by non-ASAS-SN sources that have missing or incorrect information on the latest supernovae website. Using archival classification and late-time spectra from TNS and WISeREP we have updated the classifications of SN 2016ajf, SN 2016bau, SN 2016gxp, KAIT-16az, Gaia16cbd, and SN 2016aqt, which were previously mistyped. CSS160708:151956+052419/SN 2016ehy has a redshift of $z = 0.045$ (I. Shivvers, private communication) and Gaia16alq/SN 2016dxv has a redshift of $z = 0.023$ (A. Piascik, private communication), measured from supernova lines in the spectra in both cases. Finally, based on an examination of available spectra, PS16dtm/SN 2016ezh, which was previously reported as a Type-II superluminous supernova (SLSN-II, Terreran et al. 2016b; Dong et al. 2016d), appears to be a highly unique object, possibly consistent with a SLSN-II, a tidal disruption event, or even rare AGN activity (e.g., Blanchard et al. 2017). For this reason, we include it in the catalog, but exclude it from the analyses that follow. All updated types and redshifts are reported in Table 2.

The name of the discovery group is listed for all supernovae discovered by other professional surveys. For those supernovae discovered by non-professional astronomers, we list "Amateurs" as the discovery source to differentiate these from those discovered by ASAS-SN and other professional astronomers and surveys. As in previous years, amateurs account for the largest number of bright supernova discoveries in 2016 after ASAS-SN.

As in our previous catalogs, we note in Table 2 if the ASAS-SN team independently recovered these supernovae while scanning our data. This is done to help quantify the impact ASAS-SN has on the discovery of bright supernovae in the absence of other supernovae searches.

2.3 The Host Galaxy Samples

For the host galaxies of both supernova samples, we collected Galactic extinction estimates for the direction to the host and host magnitudes spanning from the near-ultraviolet (NUV) to the infrared (IR) wavelengths. We present these data in Tables 3 and 4 for ASAS-SN hosts and non-ASAS-SN hosts, respectively. Galactic A_V from Schlafly & Finkbeiner (2011) at the positions of the supernovae were gathered from NED. NUV magnitudes are taken from the Galaxy Evolution Explorer (GALEX; Morrissey et al. 2007) All Sky Imaging Survey (AIS), optical *ugriz* magnitudes are gathered from the Sloan Digital Sky Survey Data Release 13 (SDSS DR13; SDSS Collaboration et al. 2016), NIR JHK_S magnitudes are gathered from the Two-Micron All Sky Survey (2MASS; Skrutskie et al. 2006), and IR $W1$ and $W2$ magnitudes are gathered from the Wide-field Infrared Survey Explorer (WISE; Wright et al. 2010) AllWISE source catalog.

When a host galaxy was not detected in 2MASS, we adopted an upper limit corresponding to the faintest 2MASS host magnitudes in our sample for the J and H bands ($m_J > 16.5$, $m_H > 15.7$). For hosts that are not detected in 2MASS but are detected in the WISE $W1$ band, we estimated a host magnitude by adding the mean $K_S - W1$ offset from the sample to the WISE $W1$ data. This offset was calculated by averaging the offsets for all hosts that are detected in both the K_S and $W1$ bands from both supernova samples from 2014 May 1 through 2016 December 31. The average offset is equal to -0.51 magnitudes with a scatter of 0.04 magnitudes and a standard error of 0.002 magnitudes. If a host was not detected in either 2MASS or WISE, we adopted an upper limit of $m_{K_S} > 15.6$, corresponding to the faintest detected host in our sample.

3 ANALYSIS OF THE SAMPLE

Combining all the bright supernovae discovered between 2014 May 01, when ASAS-SN became operational in both hemispheres, and 2016 December 31 provides a sample of 668 supernovae once we exclude ASAS-SN discoveries with $m_{peak} > 17.0$ (Holoien et al. 2016a, 2017). Of these, 58% (389) were discovered by ASAS-SN, 21% (137) were discovered by other professional surveys, and 21% (142) were

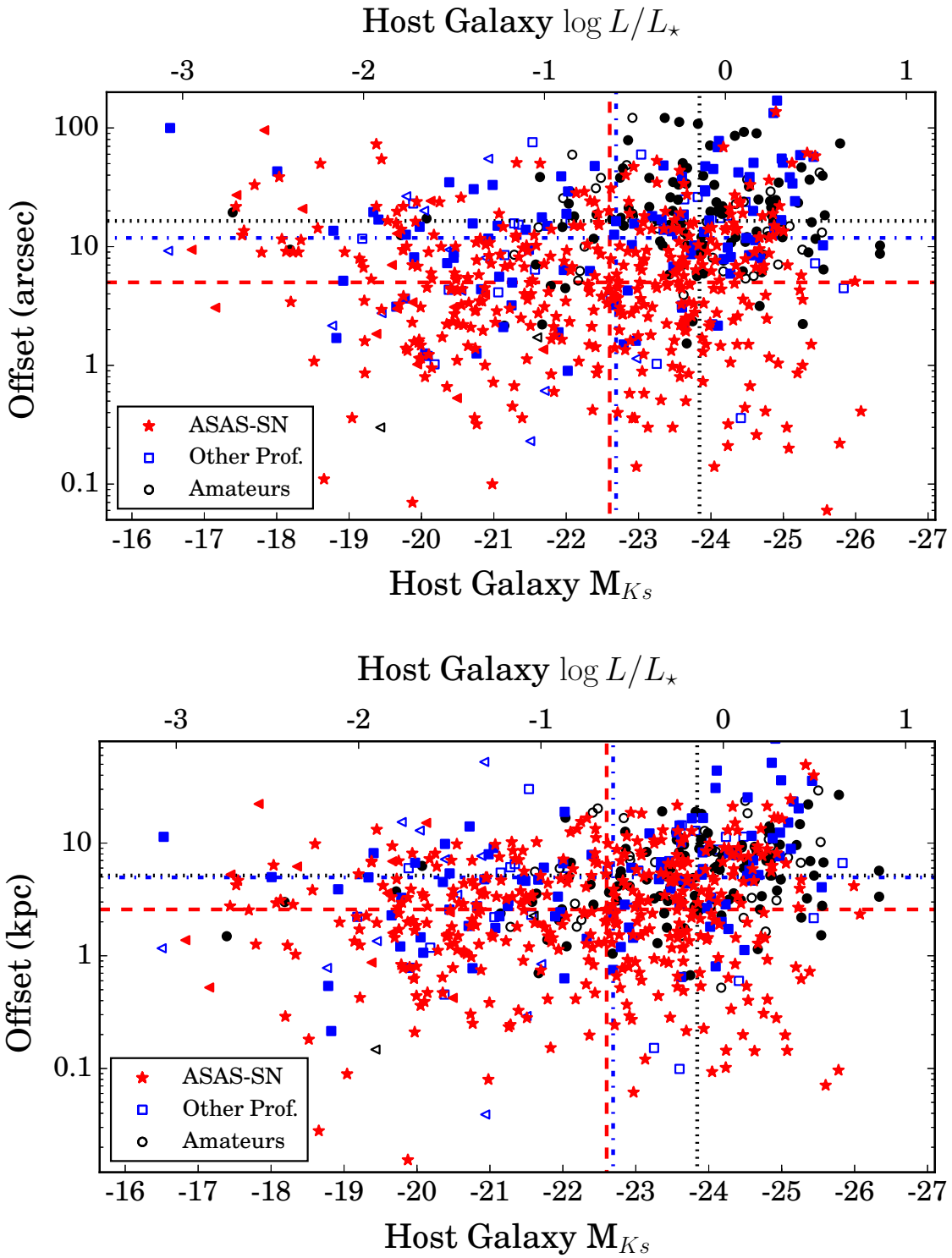

Figure 2. *Upper Panel*: Offset from the host nucleus in arcseconds compared to the absolute K_S-band host magnitude for all supernovae in our combined sample discovered between 2014 May 1 and 2016 December 31. The top axis shows $\log(L/L_\star)$ values corresponding to the magnitude range shown on the bottom scale assuming $M_{\star,K_S} = -24.2$ (Kochanek et al. 2001). ASAS-SN supernova discoveries are shown as red stars, amateur discoveries are shown as black circles, and discoveries by other professional searches are shown as blue squares. Triangles indicate upper limits on the host galaxy magnitudes for hosts that were not detected in 2MASS or WISE. Points are filled for supernovae that were independently recovered by ASAS-SN. We indicate the median offsets and host magnitudes for ASAS-SN discoveries, amateur discoveries, and other professional discoveries using dashed, dotted, and dash-dotted lines, respectively, in colors that match the data points. *Lower Panel*: As above, but with the offset measured in kiloparsecs.

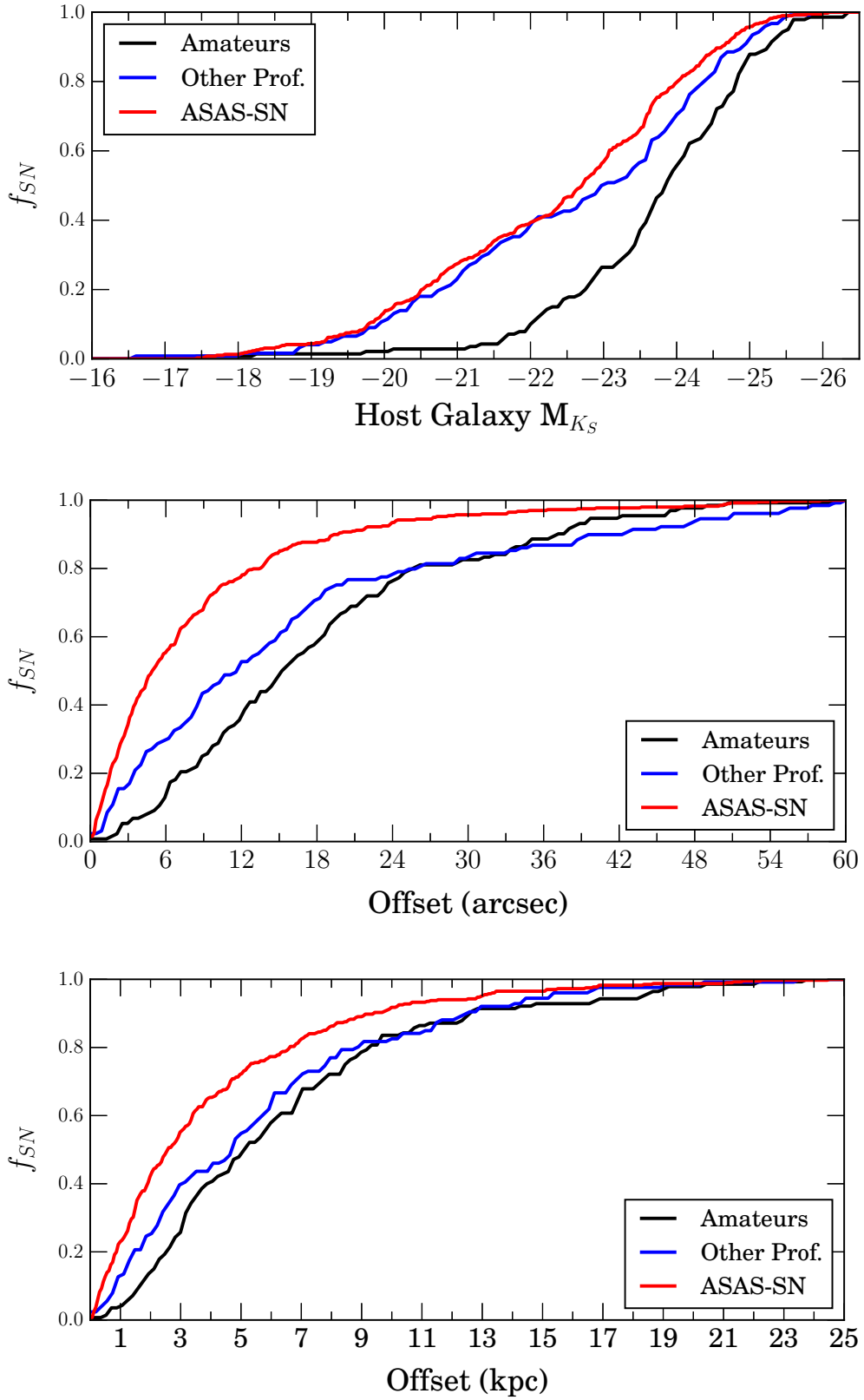

Figure 3. Cumulative, normalized distributions of host galaxy absolute magnitude (upper panel), offset from host nucleus in arcseconds (center panel), and offset from host nucleus in kpc (bottom panel) for the ASAS-SN supernova sample (red), the other professional sample (blue), and the amateur sample (black). These figures further illustrate the trends from Figure 2: Amateur discoveries are clearly more biased towards more luminous hosts than professional surveys (including ASAS-SN), while ASAS-SN finds supernovae at smaller offsets, regardless of whether offset is measured in arcseconds or kpc.

discovered by amateur astronomers. 449 were Type Ia supernovae, 178 were Type II supernovae, 40 were Type Ib/Ic supernovae, and 1 was a superluminous supernova. As in our previous catalogs, we consider Type IIb supernovae as part of the Type II sample to allow for more direct comparison with the results of Li et al. (2011). ASASSN-15lh is excluded in analyses that follow looking at trends by type, as all available evidence points to it being an extremely luminous Type I SLSN (Dong et al. 2016a; Godoy-Rivera et al. 2017), though it has also been classified as a tidal disruption event around a Kerr black hole (Leloudas et al. 2016). ASAS-SN discoveries account for 66% of the Type Ia supernovae, 45% of the Type II supernovae, and 25% of the Type Ib/Ic supernovae. Amateur discoveries account for 16%, 30%, and 48% of the Type Ia, Type II, and Type Ib/Ic supernovae in the sample, respectively, and discoveries from other professional surveys account for the remaining 18%, 25%, and 28% of each type.

Figure 1 shows pie charts breaking down the type distributions of supernovae in the ASAS-SN, non-ASAS-SN, and combined samples. Type Ia supernovae represent the largest fraction of supernovae in all three samples, as expected for a magnitude-limited sample (e.g., Li et al. 2011). Comparing to the "ideal magnitude-limited sample" breakdown predicted from the LOSS sample in Li et al. (2011), where there are 79% Type Ia, 17% Type II, and 4% Type Ib/Ic, the ASAS-SN sample matches the LOSS prediction almost exactly. The non-ASAS-SN sample and the combined sample have higher fractions of core-collapse supernovae, as was the case in our previous catalogs (Holoien et al. 2016a, 2017).

ASAS-SN continues to be the dominant source of bright supernova discoveries, and we often discover supernovae shortly after explosion due to our rapid cadence: of the 336 ASAS-SN discoveries with approximate discovery ages, 69% (232) were discovered prior to reaching their peak brightness. As was seen in Holoien et al. (2017), ASAS-SN is less affected by host galaxy selection effects than other bright supernova searches. For example, 25% (96) of the ASAS-SN bright supernovae were found in catalogued hosts that did not have previous redshift measurements available in NED, and an additional 4% (14) were discovered in uncatalogued hosts or have no apparent host galaxy. Conversely, only 16% (44) of non-ASAS-SN discoveries were found in catalogued hosts without redshift measurements, and only 3% (8) were in uncatalogued galaxies or were hostless.

As we showed in our previous catalogs, ASAS-SN discoveries have a smaller average offset from their host galaxy nuclei than bright supernovae discovered by other searches. The host galaxy K_S-band absolute magnitudes and the offsets of the supernovae from the host centers for all supernovae in our sample are shown in Figure 2. The median offsets and magnitudes are shown with horizontal and vertical lines for each supernova source (ASAS-SN, amateurs, or other professionals). A luminosity scale corresponding to the magnitude scale is given on the upper axis of the figure to help put the magnitude scale in perspective, assuming that a typical $L_\star$ galaxy has $M_{\star,K_S} = -24.2$ (Kochanek et al. 2001).

Amateur supernova searches tend to observe bright, nearby galaxies and use less sophisticated detection techniques than professional surveys, resulting in discoveries that are significantly biased towards more luminous hosts and larger offsets from the host nucleus. As we found previously (Holoien et al. 2017), other professional surveys continue to discover supernovae with smaller angular separations than amateurs (median value of $11\farcs8$ vs. $16\farcs5$), but show a similar median offset in terms of physical separation (5.0 kpc for professionals, 5.2 kpc for amateurs). ASAS-SN continues to be less biased against discoveries close to the host nucleus than either comparison group, as ASAS-SN discoveries show median offsets of $5\farcs0$ and 2.6 kpc.

These trends are more easily visible when looking at the cumulative distributions of the host galaxy magnitudes and offsets from host nuclei, as shown in Figure 3. The distributions clearly show that the ASAS-SN and other professional samples stand out from the amateur sample in host galaxy luminosity, and that supernovae discovered by ASAS-SN are more concentrated towards the centers of their hosts than those discovered by either amateurs or other professionals. While the majority of non-ASAS-SN professional discoveries continue to be made by professional searches that do not use difference imaging (e.g., MASTER, Gaia, CRTS), a larger fraction of other professional discoveries were made by surveys that do use difference imaging in 2016 than in previous years due to the start of the ATLAS survey. ASAS-SN continues to find sources with smaller median offsets than its competitors despite this fact, implying that the avoidance of the central regions of galaxies is still fairly common in surveys other than ASAS-SN, regardless of survey strategy and techniques.

The median host magnitudes are $M_{K_S} \simeq -22.6$, $M_{K_S} \simeq -22.8$, and $M_{K_S} \simeq -23.8$ for ASAS-SN discoveries, other professional discoveries, and amateur discoveries, respectively. There remains a clear distinction between professional surveys (including ASAS-SN) and amateurs in terms of host luminosity, and ASAS-SN discoveries now have a fainter median than those of other professional surveys.

As we have shown previously, one way the impact of ASAS-SN on the discovery of bright supernovae can be seen is by looking at the number of bright supernovae discovered per month in recent years (e.g., Holoien et al. 2017). In Figure 4 we show the number of supernovae with $m_{peak} \leqslant 17$ per month in each month from 2012 through 2016. Milestones in the ASAS-SN timeline, such as the deployment of our southern unit Cassius and software improvements, are shown on the figure to help visualize the impact of these hardware and software improvements.

In its first year of operation, ASAS-SN had little effect on the number of bright supernovae being discovered per month: the average number of bright supernovae discovered per month from 2012 January through 2013 May was 13 with a scatter of 4 supernovae per month, and from 2013 June through 2014 May the average was 15 with a scatter of 5 supernovae per month. However, the addition of our southern unit Cassius and improvements to our pipeline dramatically impacted our detection efficiency and survey cadence, resulting in a significant increase in the number of supernovae discovered per month: since ASAS-SN became operational in both hemispheres, the average number of bright supernova discoveries has increased to 20 with a scatter of 5 supernovae per month. This indicates that ASAS-SN has increased the rate of bright supernovae discovered per month since becoming operational in the southern hemisphere, from $\sim 13 \pm 2$

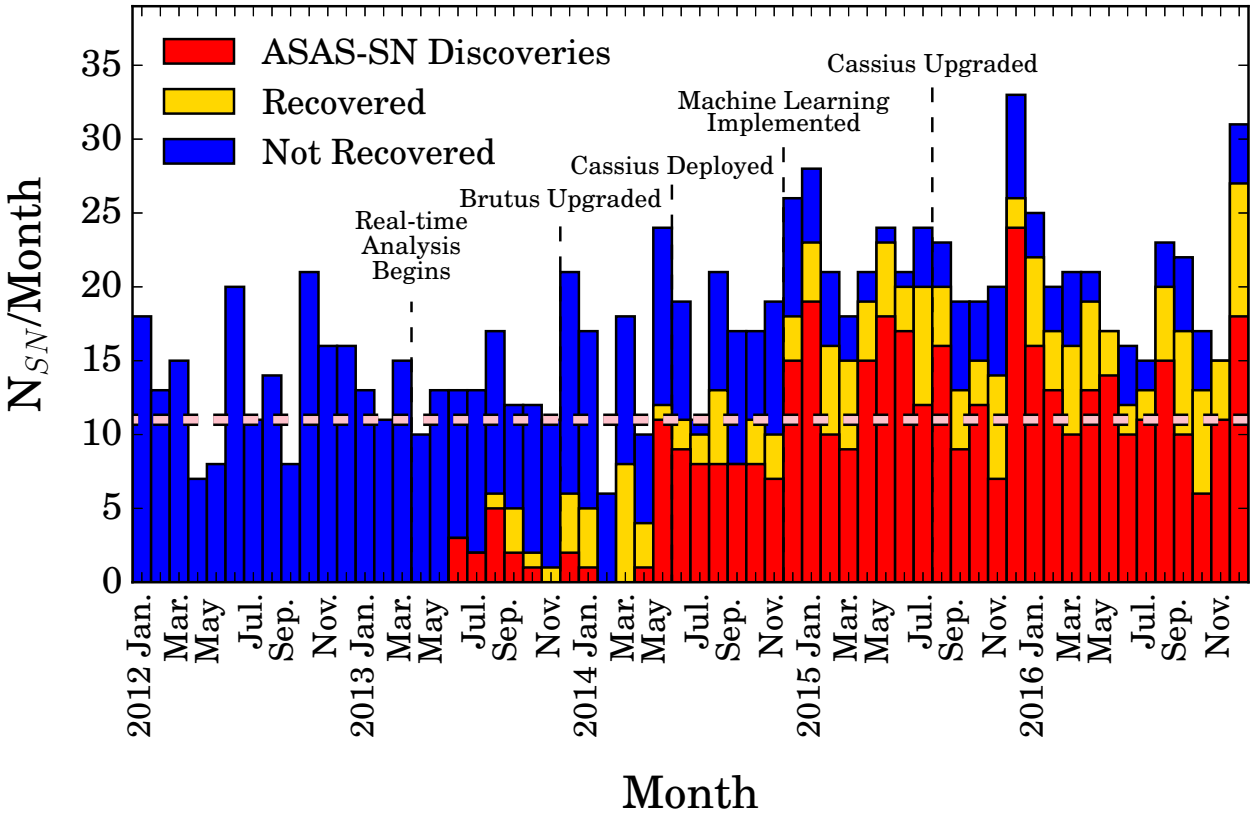

Figure 4. Histogram of bright supernova discoveries in each month from 2012 through 2016. ASAS-SN discoveries are shown in red, supernovae discovered by other sources and recovered in ASAS-SN data are shown in yellow, and supernovae that were not recovered by ASAS-SN are shown in blue. Significant milestones in the ASAS-SN timeline are also shown. The dashed pink line shows the median number of supernovae discovered in each month from 2010 through 2012. The number of bright supernova discoveries has exceeded this previous median in every month since ASAS-SN became operational in both hemispheres in 2014 May, and ASAS-SN discoveries account for at least half of all bright supernova discoveries in every month since 2014 April.

supernovae per month to $\sim 20 \pm 2$ supernovae per month, and has continued to maintain this increased rate for the last 2.5 years—the addition of the 2016 supernovae has only decreased the average number of discoveries by 1 supernova per month from the previous 2014+2015 sample (Holoien et al. 2017). ASAS-SN is discovering supernovae that otherwise would not be found, allowing us to construct a more complete sample of bright, nearby supernovae than was previously possible.

Figure 5 shows the redshift distribution of our full sample, divided by type. There is a clear distinction between the three types shown, with the Type Ia distribution peaking between $z = 0.03$ and $z = 0.035$, the Type II distribution peaking between $z = 0.01$ and $z = 0.015$, and the Type Ib/Ic distribution peaking between $z = 0.015$ and $z = 0.02$. Type Ia supernovae have a more luminous mean peak luminosity than core-collapse supernovae, so this distribution is expected for our magnitude-limited sample, and is similar to what we have seen in our previous catalogs (Holoien et al. 2016a, 2017).

Finally, we show a cumulative histogram of supernova peak magnitudes with $13.5 < m_{peak} < 17.0$ in Figure 6. As in our previous catalogs, the Figure shows ASAS-SN discoveries, ASAS-SN discoveries and supernovae recovered by ASAS-SN, and all supernovae from our sample separately. While amateur observers still account for a large number of the brightest discoveries (those with $m_{peak} \lesssim 14.5$; Holoien et al. 2017), ASAS-SN has discovered a significant fraction of these very bright supernovae in 2015 and 2016, accounting for roughly half of such discoveries in our complete sample. ASAS-SN recovers the vast majority of such very bright cases that it does not discover, showing that it is competitive with amateurs who observe the small number of very low-redshift galaxies with high cadence. ASAS-SN discovered or recovered every supernova with $m_{peak} < 14.3$ in 2016 and accounts for a large fraction of the brightest supernovae overall.

Figure 6 also illustrates an estimate of the completeness of our sample. We fit a broken power-law (shown with a green dashed line in the Figure) to the magnitudes of the observable supernovae brighter than $m_{peak} = 17.01$, assuming a Euclidean slope below the break magnitude and a variable slope for higher magnitudes. We derived the parameters of the fit using Markov Chain Monte Carlo (MCMC) methods. For only the supernovae discovered by ASAS-SN in our complete sample, the number counts are consistent with the Euclidean slope down to $m = 16.34 \pm 0.07$, similar to what we found in the 2015 sample (Holoien et al. 2017). We find break magnitudes of $m = 16.26 \pm 0.06$ and $m = 16.19 \pm 0.09$ for the sample of supernovae discovered and recovered by

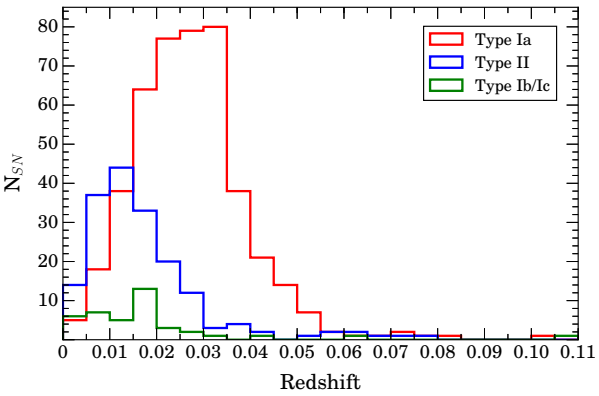

Figure 5. Histograms of supernova redshifts from our complete sample with a bin width of $z = 0.005$. Distributions for Type Ia (red line), Type II (blue line), and Type Ib/Ic (green line) supernovae are shown separately, with subtypes (such as SN 1991T-like and SN 1991bg-like Type Ia supernovae) included as part of their parent groups. As expected due to their larger intrinsic brightness, Type Ia supernovae are predominantly found at higher redshifts, while less luminous core-collapse supernovae are found at comparatively lower redshifts.

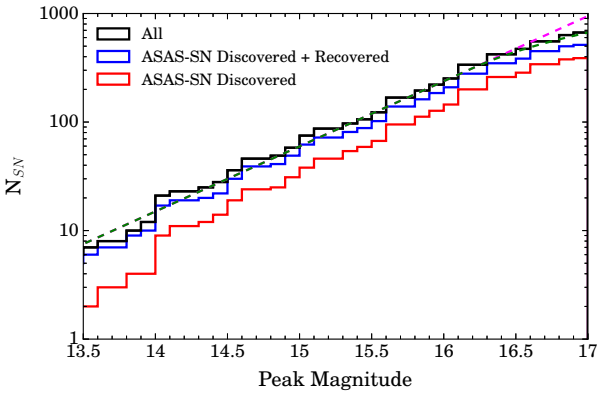

Figure 6. Cumulative histogram of supernova peak magnitudes using a 0.1 magnitude bin width. The distributions for only ASAS-SN discoveries (red line), ASAS-SN discoveries and supernovae recovered independently by ASAS-SN (blue line), and all supernovae in the sample (black line) are shown separately. The green dashed line shows a broken power-law fit that has been normalized to the complete sample with a Euclidean slope below the break magnitude and a variable slope for fainter sources, and the lavender dashed line shows an extrapolation of the Euclidean slope to $m = 17$. The sample is roughly 70% complete for $m_{peak} < 17$.

ASAS-SN and the sample of all bright supernovae, respectively, again similar to the 2015 results.

We find that the integral completenesses of the three samples relative to Euclidean predictions are 0.97 ± 0.02 (0.68 ± 0.03), 0.94 ± 0.02 (0.65 ± 0.03), and 0.93 ± 0.03 (0.71 ± 0.03) at 16.5 (17.0) mag for the ASAS-SN discovered sample, the ASAS-SN discovered + recovered sample, and the total sample, respectively. The differential completenesses relative to Euclidean predictions are 0.71 ± 0.10 (0.22 ± 0.04), 0.62 ± 0.06 (0.22 ± 0.04), and 0.67 ± 0.05 (0.36 ± 0.04) at 16.5 (17.0) mag, respectively. These results imply that roughly 70% of the supernovae brighter than $m_{peak} = 17$ are being found, and that 20−30% of the $m_{peak} = 17$ supernovae are being found, relative to the Euclidean expectation extrapolated from brighter supernovae, an improvement over the 15−20% seen in the 2015 sample. The Euclidean approximation used here does not take into account deviations from Euclidean geometry, the effects of time dilation on supernova rates, or K-corrections, and thus likely modestly underestimates the true completeness for faint supernovae. These higher order corrections will be included when we carry out a full analysis of nearby supernova rates.

4 CONCLUSIONS

This paper represents a comprehensive catalog of spectroscopically confirmed bright supernovae and their hosts from the ASAS-SN team, comprising 248 supernovae discovered by ASAS-SN, other professional surveys, and amateur observers in 2016. Our total combined bright supernova sample now includes 668 supernovae, 387 discovered by ASAS-SN. The combined sample remains similar to that of an ideal magnitude-limited sample from Li et al. (2011) with a smaller proportion of Type Ia supernova relative to core-collapse supernovae than expected.

ASAS-SN is the only professional survey that provides a complete, rapid-cadence, all-sky survey of the nearby transient Universe, and continues to have a major impact on the discovery and follow-up of bright supernovae. Even with the advent of recent professional surveys, amateur astronomers, who focus on bright and nearby galaxies for their supernova searches, remain the primary competition to ASAS-SN for new discoveries. Our analyses show that ASAS-SN continues to find supernovae that would not be found otherwise (e.g., Figure 4) and that it finds supernovae closer to galactic nuclei and in less luminous hosts than its competitors (Figure 2). In 2016 ASAS-SN recovered the majority of bright supernovae that it did not discover, as was the case in 2015, and discovered or recovered all but one of the very bright ($m_{peak} \leqslant 15$) supernovae that were discovered in 2016.

Our sample completeness is comparable to what it was at the end of 2015. Figure 6 shows that the magnitude distribution of supernovae discovered between 2014 May 1 and 2016 December 31 is roughly complete to a peak magnitude of $m_{peak} = 16.2$, slightly worse than in 2015, but that it is roughly 70% complete for $m_{peak} \leqslant 17.0$, a slight improvement over 2015. This analysis serves as a precursor to rate calculations which will be presented in Holoien et al. (*in prep.*). These rate calculations may have a significant impact on a number of fields, including the nearby core-collapse rate (e.g., Horiuchi et al. 2011, 2013) and multi-messenger studies ranging from gravitational waves (e.g., Ando et al. 2013; Nakamura et al. 2016), to MeV gamma rays from Type Ia supernovae (e.g., Horiuchi & Beacom 2010; Diehl et al. 2014; Churazov et al. 2015) to GeV–TeV gamma rays and neutrinos from rare types of core-collapse supernovae (e.g., Ando & Beacom 2005; Murase et al. 2011; Abbasi et al. 2012). Such joint measurements would be a great increase in the scientific reach of ASAS-SN discoveries.

This is the third of a yearly series of bright supernova catalogs provided by the ASAS-SN team, and it is our hope

that these catalogs will provide convenient and useful repositories of bright supernovae and their host galaxies that can be used for new and interesting population studies. ASAS-SN continues to discover many of the best and brightest transients in the sky, and these catalogs are one way in which we can use our unbiased sample to impact supernova research now and in the future.

ACKNOWLEDGMENTS

The authors thank A. Piascik and I. Shivvers for providing redshift measurements.

We thank Las Cumbres Observatory and its staff for their continued support of ASAS-SN.

ASAS-SN is supported by the Gordon and Betty Moore Foundation through grant GBMF5490 to the Ohio State University and NSF grant AST-1515927. Development of ASAS-SN has been supported by NSF grant AST-0908816, the Center for Cosmology and AstroParticle Physics at the Ohio State University, the Mt. Cuba Astronomical Foundation, the Chinese Academy of Sciences South America Center for Astronomy (CASSACA), and by George Skestos.

TW-SH is supported by the DOE Computational Science Graduate Fellowship, grant number DE-FG02-97ER25308. JSB, KZS, and CSK are supported by NSF grant AST-1515927. KZS and CSK are also supported by NSF grant AST-1515876. BJS is supported by NASA through Hubble Fellowship grant HST-HF-51348.001 awarded by the Space Telescope Science Institute, which is operated by the Association of Universities for Research in Astronomy, Inc., for NASA, under contract NAS 5-26555. Support for JLP is in part provided by FONDECYT through the grant 1151445 and by the Ministry of Economy, Development, and Tourism's Millennium Science Initiative through grant IC120009, awarded to The Millennium Institute of Astrophysics, MAS. SD and PC are supported by ?the Strategic Priority Research Program-The Emergence of Cosmological Structures? of the Chinese Academy of Sciences (Grant No. XDB09000000). SD, SB and PC are also supported by Project 11573003 supported by NSFC. JFB is supported by NSF grant PHY-1404311. JS acknowledges support from the Packard Foundation. MDS is supported by generous grants provided by the Danish Agency for Science and Technology and Innovation realized through a Sapere Aude Level 2 grant and the Villum foundation. PRW acknowledges support from the US Department of Energy as part of the Laboratory Directed Research and Development program at LANL.

This research uses data obtained through the Telescope Access Program (TAP), which has been funded by ?the Strategic Priority Research Program-The Emergence of Cosmological Structures? of the Chinese Academy of Sciences (Grant No.11 XDB09000000) and the Special Fund for Astronomy from the Ministry of Finance.

This research has made use of the XRT Data Analysis Software (XRTDAS) developed under the responsibility of the ASI Science Data Center (ASDC), Italy. At Penn State the NASA *Swift* program is support through contract NAS5-00136.

This research was made possible through the use of the AAVSO Photometric All-Sky Survey (APASS), funded by the Robert Martin Ayers Sciences Fund.

This research has made use of data provided by Astrometry.net (Barron et al. 2008; Lang et al. 2010).

This paper uses data products produced by the OIR Telescope Data Center, supported by the Smithsonian Astrophysical Observatory.

Observations made with the NASA Galaxy Evolution Explorer (GALEX) were used in the analyses presented in this manuscript. Some of the data presented in this paper were obtained from the Mikulski Archive for Space Telescopes (MAST). STScI is operated by the Association of Universities for Research in Astronomy, Inc., under NASA contract NAS5-26555. Support for MAST for non-HST data is provided by the NASA Office of Space Science via grant NNX13AC07G and by other grants and contracts.

Funding for SDSS-III has been provided by the Alfred P. Sloan Foundation, the Participating Institutions, the National Science Foundation, and the U.S. Department of Energy Office of Science. The SDSS-III web site is http://www.sdss3.org/.

This publication makes use of data products from the Two Micron All Sky Survey, which is a joint project of the University of Massachusetts and the Infrared Processing and Analysis Center/California Institute of Technology, funded by NASA and the National Science Foundation.

This publication makes use of data products from the Wide-field Infrared Survey Explorer, which is a joint project of the University of California, Los Angeles, and the Jet Propulsion Laboratory/California Institute of Technology, funded by NASA.

This research is based in part on observations obtained at the Southern Astrophysical Research (SOAR) telescope, which is a joint project of the Ministério da Ciência, Tecnologia, e Inovação (MCTI) da República Federativa do Brasil, the U.S. National Optical Astronomy Observatory (NOAO), the University of North Carolina at Chapel Hill (UNC), and Michigan State University (MSU).

This research has made use of the NASA/IPAC Extragalactic Database (NED), which is operated by the Jet Propulsion Laboratory, California Institute of Technology, under contract with NASA.

REFERENCES

Abbasi R., et al., 2012, A&A, 539, A60
Ando S., Beacom J. F., 2005, Physical Review Letters, 95, 061103
Ando S., et al., 2013, Reviews of Modern Physics, 85, 1401
Balam D. D., Graham M. L., 2016a, The Astronomer's Telegram, 8788
Balam D. D., Graham M. L., 2016b, The Astronomer's Telegram, 9016
Balam D. D., Graham M. L., 2016c, The Astronomer's Telegram, 9047
Baltay C., et al., 2013, PASP, 125, 683
Barron J. T., Stumm C., Hogg D. W., Lang D., Roweis S., 2008, AJ, 135, 414
Bersier D., 2016a, The Astronomer's Telegram, 9253
Bersier D., 2016b, The Astronomer's Telegram, 9258
Bersier D., 2016c, The Astronomer's Telegram, 9273
Bersier D., et al., 2016, The Astronomer's Telegram, 9697
Blanchard P. K., et al., 2017, preprint, (arXiv:1703.07816)
Blondin S., Tonry J. L., 2007, ApJ, 666, 1024

Bock G., et al., 2016a, The Astronomer's Telegram, 8566
Bock G., et al., 2016b, The Astronomer's Telegram, 8915
Bock G., et al., 2016c, The Astronomer's Telegram, 9091
Bock G., et al., 2016d, The Astronomer's Telegram, 9668
Bose S., Thorstensen J., Klusmeyer J., Stanek K., Prieto J., Dong S., 2016, The Astronomer's Telegram, 9405
Brimacombe J., et al., 2016a, The Astronomer's Telegram, 8539
Brimacombe J., et al., 2016b, The Astronomer's Telegram, 8542
Brimacombe J., et al., 2016c, The Astronomer's Telegram, 8652
Brimacombe J., et al., 2016d, The Astronomer's Telegram, 8685
Brimacombe J., et al., 2016e, The Astronomer's Telegram, 8703
Brimacombe J., et al., 2016f, The Astronomer's Telegram, 8712
Brimacombe J., et al., 2016g, The Astronomer's Telegram, 8897
Brimacombe J., et al., 2016h, The Astronomer's Telegram, 8898
Brimacombe J., et al., 2016i, The Astronomer's Telegram, 8979
Brimacombe J., et al., 2016j, The Astronomer's Telegram, 9005
Brimacombe J., et al., 2016k, The Astronomer's Telegram, 9057
Brimacombe J., et al., 2016l, The Astronomer's Telegram, 9058
Brimacombe J., et al., 2016m, The Astronomer's Telegram, 9117
Brimacombe J., et al., 2016n, The Astronomer's Telegram, 9123
Brimacombe J., et al., 2016o, The Astronomer's Telegram, 9188
Brimacombe J., et al., 2016p, The Astronomer's Telegram, 9199
Brimacombe J., et al., 2016q, The Astronomer's Telegram, 9212
Brimacombe J., et al., 2016r, The Astronomer's Telegram, 9262
Brimacombe J., et al., 2016s, The Astronomer's Telegram, 9270
Brimacombe J., et al., 2016t, The Astronomer's Telegram, 9305
Brimacombe J., et al., 2016u, The Astronomer's Telegram, 9332
Brimacombe J., et al., 2016v, The Astronomer's Telegram, 9338
Brimacombe J., et al., 2016w, The Astronomer's Telegram, 9344
Brimacombe J., et al., 2016x, The Astronomer's Telegram, 9430
Brimacombe J., et al., 2016y, The Astronomer's Telegram, 9439
Brimacombe J., et al., 2016z, The Astronomer's Telegram, 9457
Brimacombe J., et al., 2016aa, The Astronomer's Telegram, 9474
Brimacombe J., et al., 2016ab, The Astronomer's Telegram, 9560
Brimacombe J., et al., 2016ac, The Astronomer's Telegram, 9714
Brimacombe J., et al., 2016ad, The Astronomer's Telegram, 9724
Brimacombe J., et al., 2016ae, The Astronomer's Telegram, 9727
Brimacombe J., et al., 2016af, The Astronomer's Telegram, 9785
Brimacombe J., et al., 2016ag, The Astronomer's Telegram, 9796
Brimacombe J., et al., 2016ah, The Astronomer's Telegram, 9798
Brimacombe J., et al., 2016ai, The Astronomer's Telegram, 9804
Brimacombe J., et al., 2016aj, The Astronomer's Telegram, 9812
Brimacombe J., et al., 2016ak, The Astronomer's Telegram, 9822
Brimacombe J., et al., 2016al, The Astronomer's Telegram, 9893
Brimacombe J., et al., 2017, The Astronomer's Telegram, 9927
Brown T. M., et al., 2013, PASP, 125, 1031
Brown J. S., W.-S Holoien T., Auchettl K., Stanek K. Z., Kochanek C. S., Shappee B. J., Prieto J. L., Grupe D., 2016a, preprint, (arXiv:1609.04403)
Brown J. S., Shappee B. J., Holoien T. W.-S., Stanek K. Z., Kochanek C. S., Prieto J. L., 2016b, MNRAS, 462, 3993
Brown J. S., et al., 2016c, The Astronomer's Telegram, 8496
Brown J. S., et al., 2016d, The Astronomer's Telegram, 8537
Brown J. S., et al., 2016e, The Astronomer's Telegram, 8647
Brown J. S., et al., 2016f, The Astronomer's Telegram, 8736
Brown J. S., et al., 2016g, The Astronomer's Telegram, 8775
Brown J. S., et al., 2016h, The Astronomer's Telegram, 8885
Brown J. S., et al., 2016i, The Astronomer's Telegram, 8930
Brown J. S., et al., 2016j, The Astronomer's Telegram, 8947
Brown J. S., et al., 2016k, The Astronomer's Telegram, 9001
Brown J. S., et al., 2016l, The Astronomer's Telegram, 9127
Brown J. S., et al., 2016m, The Astronomer's Telegram, 9222
Brown J. S., et al., 2016n, The Astronomer's Telegram, 9227
Brown J. S., et al., 2016o, The Astronomer's Telegram, 9278
Brown J. S., et al., 2016p, The Astronomer's Telegram, 9341
Brown J. S., et al., 2016q, The Astronomer's Telegram, 9354
Brown J. S., et al., 2016r, The Astronomer's Telegram, 9395
Brown J. S., et al., 2016s, The Astronomer's Telegram, 9445
Brown J. S., et al., 2016t, The Astronomer's Telegram, 9484
Brown J. S., et al., 2016u, The Astronomer's Telegram, 9494
Brown J. S., et al., 2016v, The Astronomer's Telegram, 9571
Brown J. S., et al., 2016w, The Astronomer's Telegram, 9584
Brown J. S., et al., 2016x, The Astronomer's Telegram, 9601
Brown J. S., et al., 2016y, The Astronomer's Telegram, 9602
Brown J. S., et al., 2016z, The Astronomer's Telegram, 9666
Brown J. S., et al., 2016aa, The Astronomer's Telegram, 9898
Chambers K. C., et al., 2016, preprint, (arXiv:1612.05560)
Chen P., et al., 2016a, The Astronomer's Telegram, 9398
Chen P., et al., 2016b, The Astronomer's Telegram, 9407
Chornock R., et al., 2016, The Astronomer's Telegram, 8765
Churazov E., et al., 2015, ApJ, 812, 62
Cikota A., et al., 2016a, The Astronomer's Telegram, 8613
Cikota A., et al., 2016b, The Astronomer's Telegram, 9878
Cikota A., et al., 2016c, The Astronomer's Telegram, 9889
Cruz I., et al., 2016a, The Astronomer's Telegram, 8666
Cruz I., et al., 2016b, The Astronomer's Telegram, 8784
Cruz I., et al., 2016c, The Astronomer's Telegram, 8944
Cruz I., et al., 2016d, The Astronomer's Telegram, 8953
Cruz I., et al., 2016e, The Astronomer's Telegram, 9073
Diehl R., et al., 2014, Science, 345, 1162
Dimitriadis G., et al., 2016, The Astronomer's Telegram, 8555
Dong S., et al., 2016a, Science, 351, 257
Dong S., et al., 2016b, The Astronomer's Telegram, 8521
Dong S., et al., 2016c, The Astronomer's Telegram, 8892
Dong S., et al., 2016d, The Astronomer's Telegram, 9843
Drake A. J., et al., 2009, ApJ, 696, 870
Elias-Rosa N., et al., 2016a, The Astronomer's Telegram, 8727
Elias-Rosa N., et al., 2016b, The Astronomer's Telegram, 9090
Falco E., Macri L., Stringer K., Prieto J. L., Challis P., Kirshner R., 2016a, The Astronomer's Telegram, 8636
Falco E., Challis P., Kirshner R., Berlind P., Calkins M., Prieto J. L., Stanek K. Z., 2016b, The Astronomer's Telegram, 8896
Falco E., Calkins M., Challis P., Kirshner R., Prieto J. L., Stanek K. Z., 2016c, The Astronomer's Telegram, 9118
Falco E., Calkins M., Challis P., Kirshner R., Prieto J. L., Stanek K. Z., 2016d, The Astronomer's Telegram, 9219
Falco E., Calkins M., Challis P., Kirshner R., Prieto J. L., Stanek K. Z., 2016e, The Astronomer's Telegram, 9237
Faran T., et al., 2016, The Astronomer's Telegram, 8724
Fausnaugh M., et al., 2016, The Astronomer's Telegram, 9146
Fernandez J. M., et al., 2016a, The Astronomer's Telegram, 8628
Fernandez J. M., et al., 2016b, The Astronomer's Telegram, 8796
Frank S., Prieto J. L., Stanek K. Z., 2016, The Astronomer's Telegram, 8830
Fraser M., et al., 2016, The Astronomer's Telegram, 9208
Frieman J. A., et al., 2008, AJ, 135, 338
Gal-Yam A., Mazzali P. A., Manulis I., Bishop D., 2013, PASP, 125, 749
Gall C., et al., 2016, The Astronomer's Telegram, 9368
Godoy-Rivera D., et al., 2017, MNRAS, 466, 1428
Gorbovskoy E. S., et al., 2013, Astronomy Reports, 57, 233
Harmanen J., et al., 2016, The Astronomer's Telegram, 9326
Harutyunyan A. H., et al., 2008, A&A, 488, 383
Herczeg G. J., et al., 2016, preprint, (arXiv:1607.06368)
Hodgkin S. T., Wyrzykowski L., Blagorodnova N., Koposov S., 2013, Philosophical Transactions of the Royal Society of London Series A, 371, 20120239
Holoien T. W.-S., et al., 2014a, MNRAS, 445, 3263
Holoien T. W.-S., et al., 2014b, ApJ, 785, L35
Holoien T. W.-S., et al., 2016a, preprint, (arXiv:1604.00396)
Holoien T. W.-S., et al., 2016b, Acta Astron., 66, 219
Holoien T. W.-S., et al., 2016c, MNRAS, 455, 2918
Holoien T. W.-S., et al., 2016d, MNRAS, 463, 3813
Holoien T. W.-S., et al., 2016e, The Astronomer's Telegram, 8569
Holoien T. W.-S., et al., 2016f, The Astronomer's Telegram, 8614

Holoien T. W.-S., Godoy-Rivera D., Prieto J. L., 2016g, The Astronomer's Telegram, 8955
Holoien T. W.-S., et al., 2016h, The Astronomer's Telegram, 9011
Holoien T. W.-S., et al., 2016i, The Astronomer's Telegram, 9086
Holoien T. W.-S., et al., 2016j, The Astronomer's Telegram, 9195
Holoien T. W.-S., et al., 2016k, The Astronomer's Telegram, 9336
Holoien T. W.-S., et al., 2016l, The Astronomer's Telegram, 9555
Holoien T. W.-S., et al., 2016m, The Astronomer's Telegram, 9568
Holoien T. W.-S., et al., 2016n, The Astronomer's Telegram, 9825
Holoien T. W.-S., et al., 2016o, The Astronomer's Telegram, 9838
Holoien T. W.-S., et al., 2017, MNRAS,
Horiuchi S., Beacom J. F., 2010, ApJ, 723, 329
Horiuchi S., Beacom J. F., Kochanek C. S., Prieto J. L., Stanek K. Z., Thompson T. A., 2011, ApJ, 738, 154
Horiuchi S., Beacom J. F., Bothwell M. S., Thompson T. A., 2013, ApJ, 769, 113
Hosseinzadeh G., Arcavi I., McCully C., Howell D. A., Sand D., Valenti S., 2016a, The Astronomer's Telegram, 8567
Hosseinzadeh G., Yang Y., Arcavi I., Howell D. A., McCully C., Valenti S., 2016b, The Astronomer's Telegram, 8623
Hosseinzadeh G., Yang Y., Valenti S., Arcavi I., Howell D. A., McCully C., 2016c, The Astronomer's Telegram, 8679
Hosseinzadeh G., Yang Y., McCully C., Arcavi I., Howell D. A., Valenti S., 2016d, The Astronomer's Telegram, 8748
Hosseinzadeh G., Arcavi I., Yang Y., Howell D. A., Valenti S., McCully C., 2016e, The Astronomer's Telegram, 8807
Hosseinzadeh G., Arcavi I., Howell D. A., McCully C., Valenti S., 2016f, The Astronomer's Telegram, 9065
Hosseinzadeh G., Arcavi I., Howell D. A., McCully C., Valenti S., 2016g, The Astronomer's Telegram, 9589
Hosseinzadeh G., Arcavi I., Howell D. A., McCully C., Valenti S., 2016h, The Astronomer's Telegram, 9698
James P., et al., 2016, The Astronomer's Telegram, 9581
Kaiser N., et al., 2002, in Tyson J. A., Wolff S., eds, Proceedings of the SPIE Vol. 4836, Survey and Other Telescope Technologies and Discoveries. pp 154–164, doi:10.1117/12.457365
Kangas T., et al., 2016a, The Astronomer's Telegram, 9060
Kangas T., et al., 2016b, The Astronomer's Telegram, 9836
Kato T., et al., 2014a, PASJ, 66, 30
Kato T., et al., 2014b, PASJ, 66, 90
Kato T., et al., 2015, PASJ, 67, 105
Kato T., et al., 2016, PASJ, 68, 65
Kilpatrick C. D., Siebert M. R., Foley R. J., Pan Y.-C., Jha S. W., Rest A., Scolnic D., 2016a, The Astronomer's Telegram, 9361
Kilpatrick C. D., Siebert M. R., Coulter D. A., Foley R. J., Pan Y.-C., Jha S. W., Rest A., Scolnic D., 2016b, The Astronomer's Telegram, 9367
Kiyota S., et al., 2016a, The Astronomer's Telegram, 8549
Kiyota S., et al., 2016b, The Astronomer's Telegram, 8607
Kiyota S., et al., 2016c, The Astronomer's Telegram, 8621
Kiyota S., et al., 2016d, The Astronomer's Telegram, 8882
Kiyota S., et al., 2016e, The Astronomer's Telegram, 8939
Kiyota S., et al., 2016f, The Astronomer's Telegram, 9020
Kiyota S., et al., 2016g, The Astronomer's Telegram, 9045
Kiyota S., et al., 2016h, The Astronomer's Telegram, 9815
Kochanek C. S., et al., 2001, ApJ, 560, 566
Koff R. A., et al., 2016a, The Astronomer's Telegram, 8609
Koff R. A., et al., 2016b, The Astronomer's Telegram, 9194
Lang D., Hogg D. W., Mierle K., Blanton M., Roweis S., 2010, AJ, 139, 1782
Law N. M., et al., 2009, PASP, 121, 1395
Leloudas G., et al., 2016, Nature Astronomy, 1, 0002
Li W. D., et al., 2000, in Holt S. S., Zhang W. W., eds, American Institute of Physics Conference Series Vol. 522, American Institute of Physics Conference Series. pp 103–106 (arXiv:astro-ph/9912336), doi:10.1063/1.1291702
Li W., et al., 2011, MNRAS, 412, 1441
Magee M., et al., 2016, The Astronomer's Telegram, 8902
Marples P., et al., 2016a, The Astronomer's Telegram, 9393
Marples P., et al., 2016b, The Astronomer's Telegram, 9880
Marples P., et al., 2016c, The Astronomer's Telegram, 9914
Masi G., et al., 2016a, The Astronomer's Telegram, 8556
Masi G., et al., 2016b, The Astronomer's Telegram, 8565
Masi G., et al., 2016c, The Astronomer's Telegram, 8594
Masi G., et al., 2016d, The Astronomer's Telegram, 8660
Masi G., et al., 2016e, The Astronomer's Telegram, 8801
Masi G., et al., 2016f, The Astronomer's Telegram, 9114
Masi G., et al., 2016g, The Astronomer's Telegram, 9217
Masi G., et al., 2016h, The Astronomer's Telegram, 9223
Masi G., et al., 2016i, The Astronomer's Telegram, 9918
Mattila S., et al., 2016, The Astronomer's Telegram, 8992
Monard L. A. G., et al., 2016a, The Astronomer's Telegram, 8776
Monard L. A. G., et al., 2016b, The Astronomer's Telegram, 9059
Morrell N., Shappee B. J., 2016a, The Astronomer's Telegram, 9170
Morrell N., Shappee B. J., 2016b, The Astronomer's Telegram, 9300
Morrell N., Phillips M., Bose S., Dong S., Shappee B. J., 2016a, The Astronomer's Telegram, 9899
Morrell N., Phillips M., Shappee B. J., Dong S., 2016b, The Astronomer's Telegram, 9900
Morrissey P., et al., 2007, ApJS, 173, 682
Murase K., Thompson T. A., Lacki B. C., Beacom J. F., 2011, Physical Review D, 84, 043003
Nakamura K., Horiuchi S., Tanaka M., Hayama K., Takiwaki T., Kotake K., 2016, MNRAS, 461, 3296
Nicholls B., et al., 2016a, The Astronomer's Telegram, 9079
Nicholls B., et al., 2016b, The Astronomer's Telegram, 9081
Nicholls B., et al., 2016c, The Astronomer's Telegram, 9671
Nicholls B., et al., 2016d, The Astronomer's Telegram, 9713
Nicholls B., et al., 2016e, The Astronomer's Telegram, 9826
Nicholls B., et al., 2016f, The Astronomer's Telegram, 9827
Nicolas J., et al., 2016a, The Astronomer's Telegram, 9254
Nicolas J., et al., 2016b, The Astronomer's Telegram, 9349
Nicolas J., et al., 2016c, The Astronomer's Telegram, 9422
Nicolas J., et al., 2016d, The Astronomer's Telegram, 9611
Nielsen M., et al., 2016, The Astronomer's Telegram, 9630
Pan Y.-C., Downing S., Foley R. J., Jha S. W., Rest A., Scolnic D., 2016a, The Astronomer's Telegram, 8506
Pan Y.-C., Kilpatrick C. D., Siebert M. R., Foley R. J., Jha S. W., Rest A., Scolnic D., 2016b, The Astronomer's Telegram, 9333
Pan Y.-C., Duarte A. S., Foley R. J., Jha S. W., Rest A., Scolnic D., 2016c, The Astronomer's Telegram, 9696
Pan Y.-C., Foley R. J., Jha S. W., Rest A., Scolnic D., 2016d, The Astronomer's Telegram, 9904
Piascik A. S., Steele I. A., 2016a, The Astronomer's Telegram, 8505
Piascik A. S., Steele I. A., 2016b, The Astronomer's Telegram, 8560
Piascik A. S., Steele I. A., 2016c, The Astronomer's Telegram, 8634
Piascik A. S., Steele I. A., 2016d, The Astronomer's Telegram, 8794
Piascik A. S., Steele I. A., 2016e, The Astronomer's Telegram, 8798
Piascik A. S., Steele I. A., 2016f, The Astronomer's Telegram, 9221
Pignata G., et al., 2009, in Giobbi G., Tornambe A., Raimondo G., Limongi M., Antonelli L. A., Menci N., Brocato E., eds, American Institute of Physics Conference Series Vol. 1111, American Institute of Physics Conference Series. pp 551–554 (arXiv:0812.4923), doi:10.1063/1.3141608
Post R. S., et al., 2016a, The Astronomer's Telegram, 9837
Post R. S., et al., 2016b, The Astronomer's Telegram, 9875
Prieto J. L., 2016, The Astronomer's Telegram, 8867

Prieto J. L., Shappee B. J., 2016a, The Astronomer's Telegram, 8924
Prieto J. L., Shappee B. J., 2016b, The Astronomer's Telegram, 8936
Prieto J. L., et al., 2016a, preprint, (arXiv:1609.00013)
Prieto J. L., Rich J., Shappee B. J., 2016b, The Astronomer's Telegram, 8629
Prieto J. L., Morrell N., Rudie G., Shappee B. J., 2016c, The Astronomer's Telegram, 9142
Prieto J. L., Seibert M., Shappee B. J., Dong S., Stanek K. Z., 2016d, The Astronomer's Telegram, 9701
Prieto J. L., Madore B. F., Shappee B. J., Seidel M. K., Dong S., Stanek K. Z., 2016e, The Astronomer's Telegram, 9805
Prieto J. L., Seidel M. K., Shappee B. J., Stanek K. Z., 2017, The Astronomer's Telegram, 9932
Pursiainen M., et al., 2016, The Astronomer's Telegram, 9717
Quimby R. M., 2006, PhD thesis, The University of Texas at Austin
Reynolds T., et al., 2016, The Astronomer's Telegram, 9272
Romero-Cañizales C., Prieto J. L., Chen X., Kochanek C. S., Dong S., Holoien T. W.-S., Stanek K. Z., Liu F., 2016, preprint, (arXiv:1609.00010)
Rui L., Wang X., Huang F., Zhang T., Zhai M., 2016a, The Astronomer's Telegram, 8532
Rui L., Wang X., Huang F., Zhai M., Zhang T., 2016b, The Astronomer's Telegram, 8771
SDSS Collaboration et al., 2016, preprint, (arXiv:1608.02013)
Schlafly E. F., Finkbeiner D. P., 2011, ApJ, 737, 103
Schmidt S. J., et al., 2014, ApJ, 781, L24
Schmidt S. J., et al., 2016, ApJ, 828, L22
Seidel M. K., Seibert M., Morrell N., Shappee B. J., 2016, The Astronomer's Telegram, 9916
Seidel M. K., Morrell N., Shappee B. J., 2017, The Astronomer's Telegram, 9922
Shappee B. J., et al., 2014, ApJ, 788, 48
Shappee B. J., et al., 2016a, ApJ, 826, 144
Shappee B. J., et al., 2016b, The Astronomer's Telegram, 8502
Shappee B. J., et al., 2016c, The Astronomer's Telegram, 9268
Shappee B. J., Prieto J. L., Rich J., Seibert M., Madore B., Poetrodjojo H., D'Agostino J., 2016d, The Astronomer's Telegram, 9409
Shappee B. J., Prieto J. L., Rich J., Madore B., Poetrodjojo H., D'Agostino J., 2016e, The Astronomer's Telegram, 9461
Shields J., et al., 2016, The Astronomer's Telegram, 9353
Short L., et al., 2016a, The Astronomer's Telegram, 9483
Short L., et al., 2016b, The Astronomer's Telegram, 9566
Skrutskie M. F., et al., 2006, AJ, 131, 1163
Smith K. W., et al., 2016, The Astronomer's Telegram, 9886
Somero A., et al., 2016, The Astronomer's Telegram, 9734
Stone G., et al., 2016, The Astronomer's Telegram, 9887
Strader J., Prieto J. L., 2017, The Astronomer's Telegram, 9940
Strader J., Chomiuk L., Shishkovsky L., 2016a, The Astronomer's Telegram, 8880
Strader J., et al., 2016b, The Astronomer's Telegram, 8965
Strader J., Chomiuk L., Prieto J. L., 2016c, The Astronomer's Telegram, 9233
Strader J., Chomiuk L., Shishkovsky L., 2016d, The Astronomer's Telegram, 9850
Strader J., Chomiuk L., Salinas R., 2016e, The Astronomer's Telegram, 9897
Taubenberger S., et al., 2016, The Astronomer's Telegram, 8708
Terndrup D. M., Calhoun G., Cannata R., Schulze J., Dong S., Prieto J. L., 2016, The Astronomer's Telegram, 9075
Terreran G., et al., 2016a, The Astronomer's Telegram, 8694
Terreran G., et al., 2016b, The Astronomer's Telegram, 9417
Tomasella L., et al., 2016a, The Astronomer's Telegram, 8672
Tomasella L., et al., 2016b, The Astronomer's Telegram, 9024
Tomasella L., Benetti S., Cappellaro E., Elias-Rosa N., Ochner P., Pastorello A., Terreran G., Turatto M., 2016c, The Astronomer's Telegram, 9420
Tomasella L., et al., 2016d, The Astronomer's Telegram, 9610
Tonry J. L., 2011, PASP, 123, 58
Tonry J., Denneau L., Stalder B., Heinze A., Sherstyuk A., Rest A., Smith K. W., Smartt S. J., 2016, The Astronomer's Telegram, 8680
Turatto M., Benetti S., Tomasella L., Cappellaro E., Elias-Rosa N., Ochner P., Terreran G., 2016, The Astronomer's Telegram, 9829
Wiethoff W., et al., 2016, The Astronomer's Telegram, 8763
Wright E. L., et al., 2010, AJ, 140, 1868
Wyrzykowski Ł., et al., 2014, Acta Astron., 64, 197
Xiang D., Rui L., Wang X., Yang Q., Wu X., Xiao F., Fan Z., Zhang T., 2017, The Astronomer's Telegram, 9926
Xin Y.-X., Zhang J.-J., 2016, The Astronomer's Telegram, 8540
Yamanaka M., et al., 2017, ApJ, 837, 1
Yaron O., Gal-Yam A., 2012, PASP, 124, 668
Zhang J.-J., 2016, The Astronomer's Telegram, 8550
Zhang J., Zheng X., Wang X., Rui L., 2016, The Astronomer's Telegram, 9093

Table 1. ASAS-SN Supernovae

SN Name	IAU Name	Discovery Date	RA[a]	Dec.[a]	Redshift	V_{disc}[b]	V_{peak}[b]	Offset (arcsec)[c]	Type	Age at Disc.[d]	Host Name	Discovery ATel	Classification ATel
ASASSN-16aa	2016A	2016-01-02.42	08:09:14.55	+00:16:50.6	0.01738	16.8	16.4	7.99	Ia	-4	UGC 04251	Brown et al. (2016c)	Pan et al. (2016a)
ASASSN-16ab	2016B	2016-01-03.62	11:55:04.20	+01:43:07.2	0.00429	14.7	14.7	11.36	II	-4	CGCG 012-116	Shappee et al. (2016b)	Piascik & Steele (2016a)
ASASSN-16ad	2016F	2016-01-09.28	01:39:32.05	+33:49:36.3	0.01614	16.2	15.1	13.99	Ia	—	KUG 0136+335	Dong et al. (2016b)	Rui et al. (2016a)
ASASSN-16ah	2016J	2016-01-11.34	05:47:45.38	+53:36:32.3	0.02850	16.8	16.7	9.19	Ia	-8	Uncatalogued	Brimacombe et al. (2016a)	Brimacombe et al. (2016a)
ASASSN-16ai	2016I	2016-01-12.58	14:39:44.77	+23:23:42.5	0.01490	17.0	16.7	8.99	IIP	—	UGC 09450	Brown et al. (2016d)	Xin & Zhang (2016)
ASASSN-16aj	2016K	2016-01-14.21	04:21:48.21	−15:45:19.3	0.03075	17.0	14.1	8.95	Ia	-2	NGC 1562	Brimacombe et al. (2016b)	Zhang (2016)
ASASSN-16al	2016L	2016-01-15.36	15:00:27.47	−13:33:09.0	0.00930	17.0	16.5	49.94	IIP	—	UGCA 397	Kiyota et al. (2016a)	Dimitriadis et al. (2016)
ASASSN-16am	2016N	2016-01-15.36	04:45:21.28	+73:23:41.1	0.01502	17.4	17.1	14.33	II	2	CGCG 328-018	Masi et al. (2016a)	Piascik & Steele (2016b)
ASASSN-16ar	2016Z	2016-01-17.21	04:28:30.83	−17:39:23.4	0.03108	17.0	16.5	0.14	Ia	1	2MASX J04283087-1739233	Masi et al. (2016b)	Masi et al. (2016b)
ASASSN-16at	2016X	2016-01-20.59	12:55:15.50	+00:05:59.7	0.00441	15.1	14.0	73.00	II	—	UGC 08041	Bock et al. (2016a)	Hosseinzadeh et al. (2016a)
ASASSN-16av	2016ac	2016-01-18.44	11:51:28.24	+22:01:33.7	0.02567	16.5	16.0	0.26	Ia	-7	NGC 3926 NED02	Holoien et al. (2016e)	Holoien et al. (2016e)
ASASSN-16aw	2016yr	2016-01-29.27	05:39:57.45	−40:30:57.9	0.03728	17.0	16.3	61.53	Ia	-1	ESO 306-G 016	Kiyota et al. (2016b)	Cikota et al. (2016a)
ASASSN-16ax	2016ag	2016-01-26.23	01:31:23.18	+60:19:13.7	0.01870	16.0	15.7	2.24	Ia	-5	2MASX J01312331+6019128	Masi et al. (2016c)	Falco et al. (2016a)
ASASSN-16ay	2016ys	2016-01-28.41	07:12:14.35	+07:14:23.2	0.02834	16.7	16.3	14.02	Ia	-2	UGC 03738	Koff et al. (2016a)	Cikota et al. (2016a)
ASASSN-16az	2016za	2016-01-29.38	11:30:33.73	−42:33:31.4	0.03407	16.9	16.4	4.69	Ia	9	2MASX J11303364-4233359	Holoien et al. (2016f)	Prieto et al. (2016b)
ASASSN-16ba	2016zb	2016-01-29.34	09:42:29.22	−16:58:26.9	0.01392	16.8	14.9	10.06	II	5	MCG -03-25-015	Holoien et al. (2016f)	Hosseinzadeh et al. (2016b)
ASASSN-16bb	2016zc	2016-01-31.60	14:05:57.10	+43:53:02.2	0.03375	16.6	16.2	5.78	Ia-91T	-7	SDSS J140557.36+435257.2	Kiyota et al. (2016c)	Piascik & Steele (2016c)
ASASSN-16bc	2016zd	2016-02-02.28	12:05:25.83	−21:24:01.2	0.03194	17.0	16.4	14.48	Ia	-10	2MASX J12052488-2123572	Fernandez et al. (2016a)	Piascik & Steele (2016c)
ASASSN-16bg	2016acx	2016-02-06.47	12:59:25.10	+27:44:25.0	0.02022	17.4	16.8	5.68	Ia	14	2MASX J12592491+2744198	Brown et al. (2016e)	Faran et al. (2016)
ASASSN-16bl	2016adk	2016-02-08.22	11:42:26.68	−36:54:23.4	0.02955	17.3	16.8	2.28	Ia	0	2MASX J11422674-3654256	Brimacombe et al. (2016c)	Terreran et al. (2016a)

This table is available in its entirety in a machine-readable form in the online journal. A portion is shown here for guidance regarding its form and content.
[a] Right ascension and declination are given in the J2000 epoch.
[b] All magnitudes are V-band magnitudes from ASAS-SN.
[c] Offset indicates the offset of the SN in arcseconds from the coordinates of the host nucleus, taken from NED.
[d] Discovery ages are given in days relative to peak. All ages are approximate and are only listed if a clear age was given in the classification telegram.

Table 2. Non-ASAS-SN Supernovae

SN Name	IAU Name[a]	Discovery Date	RA[b]	Dec.[b]	Redshift	m_{peak}[c]	Offset (arcsec)[d]	Type	Host Name	Discovered By[e]	Recovered?[f]
2016D	2016D	2016-01-01.55	04:01:25.99	−54:45:30.8	0.04510	16.5	2.23	Ia	2MASX J04012613-5445295	Amateurs	Yes
2016C	2016C	2016-01-03.84	13:38:05.30	−17:51:15.3	0.00452	14.9	112.25	IIP	NGC 5247	Amateurs	Yes
MASTER OT J165420.77-615258	—	2016-01-06.00	16:54:20.77	−61:52:58.0	0.01505	16.9	8.04	IIP	ESO 138-G006	MASTER	No
2016G	2016G	2016-01-09.94	03:03:57.74	+43:24:03.5	0.00915	16.3	16.68	Ic-BL	NGC 1171	Amateurs	Yes
2016P	2016P	2016-01-19.19	13:57:31.10	+06:05:51.0	0.01462	16.0	21.88	Ic-BL	NGC 5374	Amateurs	Yes
2016W	2016W	2016-01-20.49	02:30:39.69	+42:14:08.9	0.01925	16.0	18.44	Ia	NGC 946	Amateurs	Yes
ATLAS16aaf	2016ado	2016-01-20.78	02:03:05.79	−03:50:28.0	0.04248	17.0	3.18	Ia-07if	2MASX J02030578-0350240	ATLAS	No
ATLAS16aab	2016adp	2016-01-21.81	03:21:42.43	+42:05:49.4	0.01800	16.5	6.36	Ia-91bg	2MASX J03214217+4205549	ATLAS	No
MASTER OT J105908.57+103834.8	—	2016-01-31.06	10:59:08.57	+10:38:34.8	0.03500	16.8	5.16	Ia	SDSS J105908.63+103829.7	MASTER	Yes
2016adi	2016adi	2016-02-03.54	13:47:43.11	−30:55:57.0	0.01490	15.3	46.56	Ia	NGC 5292	Amateurs	No
2016adj	2016adj	2016-02-08.56	13:25:24.12	−43:00:57.9	0.00183	14.3	39.56	IIb	NGC 5128	Amateurs	No
2016afa	2016afa	2016-02-12.92	15:36:32.47	+16:36:36.7	0.00653	16.8	12.45	II	NGC 5962	Amateurs	Yes
2016ajf	2016ajf	2016-02-18.44	03:19:54.47	+41:33:53.5	0.02031	16.9	6.42	Ia	NGC 1278	Amateurs	Yes
Gaia16aeu	2016ajm	2016-02-20.09	02:49:36.01	−31:13:23.9	0.02136	16.9	14.70	Ia-91bg	2dFGRS S394Z183	Gaia	No
Gaia16agf	2016aqs	2016-02-27.28	06:34:08.98	−25:11:04.6	0.03000	17.0	20.09	Ia	Uncatalogued	Gaia	Yes
PS16bdu	2016bdu	2016-02.28.62	13:10:13.95	+32:31:14.1	0.01700	16.5	2.16	IIn	SDSS J131014.04+323115.9	Pan-STARRS	Yes
2016bam	2016bam	2016-03-07.43	07:46:52.72	+39:01:21.8	0.01350	15.8	33.80	II	NGC 2444	Amateurs	Yes
ATLAS16ago	2016bev	2016-03-10.33	07:47:50.21	−18:44:12.8	0.01080	16.7	50.82	IIP	ESO 560-G013	ATLAS	No
2016bas	2016bas	2016-03-12.51	07:38:05.53	−55:11:47.0	0.00941	16.8	20.02	IIb	ESO 163-G011	Amateurs	No
2016bau	2016bau	2016-03-13.97	11:20:59.02	+53:10:25.6	0.00386	14.6	38.07	Ib	NGC 3631	Amateurs	Yes

This table is available in its entirety in a machine-readable form in the online journal. A portion is shown here for guidance regarding its form and content.
[a] IAU name is not provided if one was not given to the supernova. In some cases the IAU name may also be the primary supernova name.
[b] Right ascension and declination are given in the J2000 epoch.
[c] All magnitudes are taken from D. W. Bishop's Bright Supernova website, as described in the text, and may be from different filters.
[d] Offset indicates the offset of the SN in arcseconds from the coordinates of the host nucleus, taken from NED.
[e] "Amateurs" indicates discovery by any number of non-professional astronomers, as described in the text.
[f] Indicates whether the supernova was independently recovered in ASAS-SN data or not.

Table 3. ASAS-SN Supernova Host Galaxies

Galaxy Name	Redshift	SN Name	SN Type	SN Offset (arcsec)	A_V [a]	m_{NUV} [b]	m_u [c]	m_g [c]	m_r [c]	m_i [c]	m_z [c]	m_J [d]	m_H [d]	m_{K_S} [d,e]	m_{W1}	m_{W2}
UGC 04251	0.01738	ASASSN-16aa	Ia	7.99	0.124	—	18.37 0.02	16.41 0.00	15.59 0.00	15.11 0.00	14.73 0.00	11.55 0.03	10.85 0.03	10.57 0.05	10.81 0.02	10.75 0.02
PGC 037392	0.00429	ASASSN-16ab	II	11.36	0.058	16.56 0.02	16.05 0.01	15.21 0.00	14.92 0.00	14.78 0.00	14.67 0.01	13.91 0.09	13.34 0.10	13.02 0.16	13.69 0.03	13.57 0.04
KUG 0136+335	0.01614	ASASSN-16ad	Ia	13.99	0.134	17.82 0.03	16.93 0.05	15.83 0.01	15.38 0.01	15.14 0.02	14.98 0.08	15.20 0.08	14.49 0.11	14.54 0.20	14.21 0.03	14.03 0.04
Uncatalogued	0.02850	ASASSN-16ah	Ia	9.19	0.719	20.34 0.25	—	—	—	—	—	>16.5	>15.7	14.09 0.06*	14.63 0.04	14.39 0.06
UGC 09450	0.01490	ASASSN-16ai	IIP	8.99	0.088	17.61 0.06	17.31 0.02	16.38 0.01	16.08 0.01	15.87 0.01	16.06 0.03	16.09 0.10	15.66 0.15	15.78 0.19	15.62 0.04	15.29 0.08
NGC 1562	0.03075	ASASSN-16aj	Ia	8.95	0.090	20.02 0.17	—	—	—	—	—	12.08 0.03	11.37 0.04	11.08 0.06	11.37 0.02	11.44 0.02
UGCA 397	0.00930	ASASSN-16al	IIP	49.94	0.276	16.89 0.04	—	—	—	—	—	>16.5	>15.7	14.44 0.06*	14.98 0.04	14.86 0.09
CGCG 328-018	0.01502	ASASSN-16am	II	14.33	0.470	20.49 0.18	—	—	—	—	—	11.63 0.03	10.91 0.04	10.67 0.05	11.21 0.02	11.28 0.02
2MASX J04283087-1739233	0.03108	ASASSN-16ar	Ia	0.14	0.105	—	—	—	—	—	—	12.62 0.03	11.97 0.05	11.66 0.07	11.89 0.02	11.93 0.02
UGC 08041	0.00441	ASASSN-16at	II	73.00	0.061	14.57 0.01	15.72 0.01	14.10 0.00	13.48 0.00	13.23 0.00	13.25 0.01	12.92 0.05	12.32 0.07	12.04 0.11	13.01 0.03	13.03 0.03
NGC 3926 NED02	0.02567	ASASSN-16av	Ia	0.26	0.075	19.11 0.09	16.12 0.01	14.27 0.00	13.38 0.00	12.99 0.00	12.67 0.00	11.65 0.02	10.97 0.03	10.65 0.03	11.13 0.02	11.22 0.02
ESO 306-G 016	0.03728	ASASSN-16aw	Ia	61.53	0.088	—	—	—	—	—	—	11.80 0.03	11.07 0.03	10.78 0.06	11.32 0.02	11.32 0.02
2MASX J01312331+6019128	0.01870	ASASSN-16ax	Ia	2.24	1.512	—	—	—	—	—	—	12.47 0.03	11.65 0.03	11.36 0.05	11.44 0.02	11.46 0.02
UGC 03738	0.02834	ASASSN-16ay	Ia	14.02	0.189	—	—	—	—	—	—	12.52 0.04	11.83 0.05	11.55 0.08	11.95 0.02	11.99 0.02
2MASX J11303364-4233359	0.03407	ASASSN-16az	Ia	4.69	0.235	—	—	—	—	—	—	13.57 0.05	12.87 0.05	12.53 0.08	12.50 0.02	12.49 0.02
MCG -03-25-015	0.01392	ASASSN-16ba	II	10.06	0.180	16.85 0.03	—	—	—	—	—	>16.5	>15.7	14.12 0.06*	14.66 0.03	14.58 0.06
SDSS J140557.36+435257.2	0.03375	ASASSN-16bb	Ia-91T	5.78	0.020	18.89 0.08	18.31 0.04	17.29 0.01	16.96 0.01	16.76 0.01	16.71 0.08	>16.5	>15.7	15.06 0.06*	15.60 0.04	15.40 0.08
2MASX J12052488-2123572	0.03194	ASASSN-16bc	Ia	14.48	0.152	18.26 0.06	—	—	—	—	—	12.78 0.04	12.11 0.04	11.76 0.07	11.99 0.02	11.58 0.02
2MASX J12592491+2744198	0.02022	ASASSN-16bg	Ia	5.68	0.024	20.94 0.26	17.65 0.01	15.86 0.00	15.05 0.00	14.65 0.00	14.35 0.00	13.30 0.03	12.55 0.04	12.35 0.05	12.33 0.02	12.43 0.02
2MASX J11422674-3654256	0.02955	ASASSN-16bl	Ia	2.28	0.318	—	—	—	—	—	—	12.72 0.04	11.92 0.04	11.63 0.07	11.81 0.02	11.83 0.02

This table is available in its entirety in a machine-readable form in the online journal. A portion is shown here for guidance regarding its form and content.
Uncertainty is given for all magnitudes, and in some cases is equal to zero.
[a] Galactic extinction taken from Schlafly & Finkbeiner (2011).
[b] No magnitude is listed for those galaxies not detected in GALEX survey data.
[c] No magnitude is listed for those galaxies not detected in SDSS data or those located outside of the SDSS footprint.
[d] For those galaxies not detected in 2MASS data, we assume an upper limit of the faintest galaxy detected in each band from our sample.
[e] K_S-band magnitudes marked with a "*" indicate those estimated from the WISE $W1$-band data, as described in the text.

Table 4. Non-ASAS-SN Supernova Host Galaxies

Galaxy Name	Redshift	SN Name	SN Type	SN Offset (arcsec)	A_V [a]	m_{NUV} [b]	m_u [c]	m_g [c]	m_r [c]	m_i [c]	m_z [c]	m_J [d]	m_H [d]	m_{K_S} [d,e]	m_{W1}	m_{W2}
2MASX J04012613-5445295	0.04510	2016D	Ia	2.23	0.035	19.96 0.18	—	—	—	—	—	12.34 0.03	11.63 0.04	11.26 0.06	11.49 0.02	11.55 0.02
NGC 5247	0.00452	2016C	IIP	112.25	0.244	—	—	—	—	—	—	8.80 0.02	8.17 0.02	7.93 0.03	10.46 0.02	10.34 0.02
ESO 138-G006	0.01505	MASTER J165420.77	IIP	8.04	0.425	—	—	—	—	—	—	>16.5	>15.7	13.57 0.07*	14.21 0.04	14.00 0.04
NGC 1171	0.00915	2016G	Ic-BL	16.68	0.431	15.89 0.02	15.31 0.01	13.54 0.00	12.64 0.00	12.18 0.00	11.84 0.00	10.79 0.02	10.10 0.02	9.80 0.03	10.87 0.02	10.89 0.02
NGC 5374	0.01462	2016P	Ic-BL	21.88	0.074	15.12 0.01	14.52 0.01	13.31 0.00	12.53 0.00	12.13 0.00	11.82 0.00	10.81 0.03	10.16 0.04	9.88 0.06	10.86 0.02	10.67 0.02
NGC 946	0.01925	2016W	Ia	18.44	0.191	18.83 0.12	—	—	—	—	—	10.83 0.02	10.11 0.02	9.82 0.02	10.25 0.02	10.25 0.02
2MASX J02030578-0350240	0.04248	ATLAS16aaf	Ia-07if	3.18	0.069	20.06 0.11	17.59 0.02	15.92 0.00	15.26 0.00	14.93 0.00	14.71 0.00	13.76 0.04	13.07 0.05	12.80 0.07	12.85 0.04	12.83 0.04
2MASX J03214217+4205549	0.01800	ATLAS16aab	Ia-91bg	6.36	0.513	—	18.14 0.03	16.30 0.00	15.37 0.00	14.90 0.00	14.53 0.01	13.62 0.05	12.87 0.07	12.58 0.09	13.16 0.04	13.20 0.04
SDSS J105908.63+103829.7	0.03500	MASTER J105908.57	Ia	5.16	0.069	21.29 0.22	21.31 0.32	20.18 0.05	19.77 0.06	19.57 0.06	19.93 0.32	>16.5	>15.7	16.92 0.22*	17.56 0.21	16.49 0.29
NGC 5292	0.01490	2016adi	Ia	46.56	0.164	15.76 0.02	—	—	—	—	—	9.78 0.02	9.13 0.03	8.84 0.03	10.07 0.02	10.12 0.02
NGC 5128	0.00183	2016adj	IIb	39.56	0.315	—	—	—	—	—	—	5.03 0.02	4.31 0.02	3.99 0.02	5.26 0.05	4.76 0.04
NGC 5962	0.00653	2016afa	II	12.45	0.149	14.11 0.01	13.89 0.00	12.27 0.00	11.51 0.00	11.14 0.00	10.69 0.00	9.58 0.01	8.89 0.01	8.61 0.02	9.67 0.02	9.53 0.02
NGC 1278	0.02031	2016ajf	Ia	6.42	0.451	19.11 0.05	—	—	—	—	—	10.30 0.02	9.57 0.02	9.25 0.03	10.10 0.02	10.14 0.02
2dFGRS S394Z183	0.02136	Gaia16aeu	Ia-91bg	14.70	0.069	20.43 0.13	—	—	—	—	—	>16.5	>15.7	14.77 0.07*	15.41 0.04	15.80 0.11
Uncatalogued	0.03000	Gaia16agf	Ia	20.09	0.182	—	—	—	—	—	—	>16.5	>15.7	>15.6	—	—
SDSS J131014.04+323115.9	0.01700	PS16bdu	IIn	2.16	0.041	—	22.08 0.28	21.19 0.06	20.94 0.07	20.99 0.11	21.07 0.39	>16.5	>15.7	>15.6	—	—
NGC 2444	0.01350	2016bam	II	33.80	0.140	—	15.57 0.01	13.73 0.00	12.84 0.00	12.41 0.00	12.10 0.00	11.17 0.02	10.47 0.02	10.21 0.03	10.39 0.02	10.48 0.02
ESO 560-G013	0.01080	ATLAS16ago	IIP	50.82	1.050	—	—	—	—	—	—	10.09 0.02	9.26 0.02	8.90 0.02	10.45 0.02	10.27 0.02
ESO 163-G011	0.00941	2016bas	IIb	20.02	0.407	—	—	—	—	—	—	10.81 0.02	10.01 0.02	9.64 0.03	10.32 0.02	10.08 0.02
NGC 3631	0.00386	2016bau	Ib	38.07	0.045	13.14 0.00	—	—	—	—	—	9.30 0.02	8.61 0.02	8.38 0.02	9.89 0.02	9.78 0.02

This table is available in its entirety in a machine-readable form in the online journal. A portion is shown here for guidance regarding its form and content.
Uncertainty is given for all magnitudes, and in some cases is equal to zero. "MASTER" supernova names have been abbreviated for space reasons.
[a] Galactic extinction taken from Schlafly & Finkbeiner (2011).
[b] No magnitude is listed for those galaxies not detected in GALEX survey data.
[c] No magnitude is listed for those galaxies not detected in SDSS data or those located outside of the SDSS footprint.
[d] For those galaxies not detected in 2MASS data, we assume an upper limit of the faintest galaxy detected in each band from our sample.
[e] K_S-band magnitudes marked with a "*" indicate those estimated from the WISE $W1$-band data, as described in the text.